A Pair of Hybrid Symmetrical Condensed TLM Nodes

Pierre Berini, *Student Member, IEEE*, and Ke Wu, *Senior Member, IEEE*

***Abstract*—This letter reports the development of a new time-domain hybrid symmetrical condensed TLM node. The new node can accommodate a graded mesh and model lossy anisotropic media described by diagonal tensors. The generalisation of an existing hybrid node to accommodate anisotropic media is also presented. The two hybrid nodes are complementary and provide the same computational advantages over the symmetrical condensed node originally proposed by Johns [1].**

I. Introduction

In a hybrid symmetrical condensed node (HSCN), the characteristic impedance of the link lines are varied to account for mesh grading and to model certain properties of the medium. This has the desirable effect of reducing the total number of stubs required by a generalised SCN and, in certain instances, increasing the TLM time step compared to the stub-loaded SCN originally proposed by Johns [1]. The maximum TLM time step for the HSCN's is related to the minimum node dimension while the maximum TLM time step using Johns's SCN is dependant on the ratio of the largest to the smallest grid dimension. The disadvantage of a hybrid node is that scattering may take place at the connection between link lines of neighboring nodes.

A parallel 2-D graded hybrid node was originally proposed by Al-Mukhtar and Sitch [2], and the first 3-D HSCN was reported by Scaramuzza and Lowery [3]. In both Al-Mukhtar and Scaramuzza's nodes, the characteristic admittance of the link lines model the permeability of the medium and parallel open-circuit stubs are used to model the permittivity; this type of node will be referred to as a **type I** HSCN. Alternatively, the characteristic impedance of the link lines could be varied to model the permittivity of the medium and series short-circuit stubs could be used to model the permeability; this type of node will be referred to as a **type II** HSCN. In this paper, the development of a generalized type II HSCN is presented, the type I HSCN is extended to include anisotropic media, and numerical results obtained using the time domain TLM method compare the two HSCN's, Johns's SCN [1], [4], [5] and analytic solutions.

II. Formulation

Both HSCN's presented in this paper share the geometry and the numbering scheme of the node given in [1], [4], [5]. The scattering of the voltage pulses at the center of the HSCN's is represented by the matrix S_v given at the bottom of the next page. The elements of this matrix are obtained using the technique presented in references [6], [7], [8] and are given below for both HSCN's.

Manuscript received March 17, 1994. This work was supported by FCAR.

P. Berini and K. Wu are with POLY-GRAMES, Département de génie électrique et informatique, École Polytechnique de Montréal, Montréal, Quebec, Canada H3C 3A7.

IEEE Log Number 9402969.

A. Type I Hybrid Symmetrical Condensed Node

The type I HSCN models a diagonal permeability tensor via the distributed inductance of the link lines, while the distributed capacitance is chosen such that time synchronism is maintained throughout the mesh. The characteristic admittance of the link lines thus become a function of both the permeability to be modelled and the grading of the mesh:

$$Y_x = \frac{\Delta_l \Delta_x}{\mu_{xx,r}\Delta_y\Delta_z},\quad Y_y = \frac{\Delta_l \Delta_y}{\mu_{yy,r}\Delta_x\Delta_z},\quad Y_z = \frac{\Delta_l \Delta_z}{\mu_{zz,r}\Delta_x\Delta_y} \tag{1}$$

The normalized characteristic admittance Y_x is associated with lines 4, 8, 5, and 7; Y_y with lines 2, 9, 6, and 10 and Y_z with lines 3, 11, 12, and 1.

The additional capacitance required to model the permittivity tensor is provided via the open-circuit stubs that couple to the electric field. The normalized characteristic admittance of these stubs are:

$$Yo_x = 4\epsilon_{xx,r}\frac{\Delta_y\Delta_z}{\Delta_l\Delta_x} - 2\Delta_l\left(\frac{\Delta_y}{\mu_{yy,r}\Delta_x\Delta_z} + \frac{\Delta_z}{\mu_{zz,r}\Delta_x\Delta_y}\right) \tag{2}$$

$$Yo_y = 4\epsilon_{yy,r}\frac{\Delta_x\Delta_z}{\Delta_l\Delta_y} - 2\Delta_l\left(\frac{\Delta_x}{\mu_{xx,r}\Delta_y\Delta_z} + \frac{\Delta_z}{\mu_{zz,r}\Delta_x\Delta_y}\right) \tag{3}$$

$$Yo_z = 4\epsilon_{zz,r}\frac{\Delta_x\Delta_y}{\Delta_l\Delta_z} - 2\Delta_l\left(\frac{\Delta_x}{\mu_{xx,r}\Delta_y\Delta_z} + \frac{\Delta_y}{\mu_{yy,r}\Delta_x\Delta_z}\right) \tag{4}$$

The elements of S_v are found to be:

$$a_{pq} = \frac{Y_q}{Y_r}b_{pq} - d_{pq},\quad c_{pq} = \frac{Y_q}{Y_r}b_{pq} + d_{pq} - 1$$

$$k_{pq} = e_{pq} = b_{pq} = \frac{2Y_r}{Yo_p + Go_p + 2(Y_r + Y_q)}$$

$$d_{pq} = \frac{2}{4 + Y_q Rs_q}$$

$$l_{pq} = g_{pq} = \frac{Yo_p}{Y_r}b_{pq},\quad h_{pq} = \frac{Yo_p - Go_p - 2(Y_r + Y_q)}{Yo_p + Go_p + 2(Y_r + Y_q)}$$

$$m_{pq} = Y_q Rs_q d_{pq},\quad f_{pq} = i_{pq} = j_{pq} = n_{pq} = 0$$

The type I HSCN reduces to the node given in [9] if the medium is isotropic and to the node given in [3] if the medium is both isotropic and magnetically lossless.

1051-8207/94$04.00 © 1994 IEEE

B. Type II Hybrid Symmetrical Condensed Node

The type II HSCN models a diagonal permittivity tensor via the distributed capacitance of the link lines, while the distributed inductance is chosen such that time synchronism is maintained throughout the mesh. The characteristic impedance of the link lines thus become a function of both the permittivity to be modelled and the grading of the mesh. They can be obtained from (1) by making the following textual substitutions: $Y \rightarrow Z$ and $\mu \rightarrow \epsilon$. The normalized characteristic impedance Z_x is associated with lines 1, 12, 2, and 9; Z_y with lines 4, 8, 3, and 11 and Z_z with lines 6, 10, 5, and 7.

The additional inductance required to model the permeability tensor is provided via the short-circuit stubs that couple to the magnetic field. The normalized characteristic impedance of these stubs are obtained from (2)–(4) by making the following textual substitutions: $Yo \rightarrow Zs$, $\epsilon \rightarrow \mu$ and $\mu \rightarrow \epsilon$.

The elements of S_v are found to be:

$$a_{pq} = b_{pq} - d_{pq}, \quad c_{pq} = b_{pq} + d_{pq} - 1$$

$$k_{pq} = b_{pq} = \frac{2}{4 + Z_p Go_p}$$

$$i_{pq} = d_{pq} = \frac{2Z_p}{Zs_q + Rs_q + 2(Z_r + Z_p)}$$

$$f_{pq} = \frac{Zs_q}{Z_p} d_{pq}, \quad j_{pq} = \frac{-Zs_q + Rs_q + 2(Z_r + Z_p)}{Zs_q + Rs_q + 2(Z_r + Z_p)}$$

$$n_{pq} = m_{pq} = \frac{Rs_q}{Z_p} d_{pq}, \quad e_{pq} = g_{pq} = h_{pq} = l_{pq} = 0$$

C. Commonalities

For both HSCN's, the indices p, q, r are defined as: $p, q, r \in \{x, y, z\}$ and $r \neq p, q$ where x, y, z are subscripts of the elements of S_v. The length Δ_l is chosen as the minimum of all node dimensions $\Delta_l = min\{\Delta_x, \Delta_y, \Delta_z\}_{(i,j,k)}$; this will ensure that all open- or short-circuit stubs have a positive characteristic admittance or impedance. The time step for both HSCN's is dependant on the minimum mesh dimension Δ_l and not on the ratio of the largest to the smallest grid spacing, which sometimes leads to prohibitively small time steps [3]. Assuming that the grading is constant throughout the structure, then scattering at the connection between link lines will not occur in the type I HSCN if the permeability is constant or, in the type II HSCN, if the permittivity is constant.

Parallel and series matched stubs are used to model the electric and magnetic losses of the medium. The normalized characteristic admittance of the parallel loss stubs are:

$$Go_x = \sigma_{ex} \frac{\Delta_y \Delta_z}{\Delta_x} \frac{1}{Y_0}, \quad Go_y = \sigma_{ey} \frac{\Delta_x \Delta_z}{\Delta_y} \frac{1}{Y_0}$$

$$Go_z = \sigma_{ez} \frac{\Delta_x \Delta_y}{\Delta_z} \frac{1}{Y_0}$$

The normalized characteristic impedance of the series loss stubs can be obtained from the above equations by making the following textual substitutions: $Go \rightarrow Rs$, $\sigma_e \rightarrow \sigma_m$ and $Y_0 \rightarrow Z_0$. σ_e and σ_m are the equivalent electric and magnetic conductivities and $Z_0 = 1/Y_0 = \sqrt{\mu_0/\epsilon_0}$.

III. Numerical Results

A. TEM Wave Propagation

Fig. 1 shows a transverse electromagnetic wave normally incident upon a lossy half space. We note the excellent agreement between the results obtained via the TLM method

$S_v =$

	1	2	3	4	5	6	7	8	9	10	11	12	13	14	15	16	17	18
1	a_{xz}	b_{xz}	d_{xz}						b_{xz}		$-d_{xz}$	c_{xz}	g_{xz}					i_{xz}
2	b_{xy}	a_{xy}				d_{xy}			c_{xy}	$-d_{xy}$		b_{xy}	g_{xy}				$-i_{xy}$	
3	d_{yz}		a_{yz}	b_{yz}				b_{yz}			c_{yz}	$-d_{yz}$		g_{yz}				$-i_{yz}$
4			b_{yx}	a_{yx}	d_{yx}		$-d_{yx}$	c_{yx}			b_{yx}			g_{yx}		i_{yx}		
5				d_{zx}	a_{zx}	b_{zx}	c_{zx}	$-d_{zx}$		b_{zx}					g_{zx}	$-i_{zx}$		
6		d_{zy}			b_{zy}	a_{zy}	b_{zy}		$-d_{zy}$	c_{zy}					g_{zy}		i_{zy}	
7				$-d_{zx}$	c_{zx}	b_{zx}	a_{zx}	d_{zx}		b_{zx}					g_{zx}	i_{zx}		
8			b_{yx}	c_{yx}	$-d_{yx}$		d_{yx}	a_{yx}			b_{yx}			g_{yx}		$-i_{yx}$		
9	b_{xy}	c_{xy}				$-d_{xy}$			a_{xy}	d_{xy}		b_{xy}	g_{xy}				i_{xy}	
10		$-d_{zy}$			b_{zy}	c_{zy}	b_{zy}		d_{zy}	a_{zy}					g_{zy}		$-i_{zy}$	
11	$-d_{yz}$		c_{yz}	b_{yz}				b_{yz}			a_{yz}	d_{yz}		g_{yz}				i_{yz}
12	c_{xz}	b_{xz}	$-d_{xz}$						b_{xz}		d_{xz}	a_{xz}	g_{xz}					$-i_{xz}$
13	e_{xy}	e_{xz}							e_{xz}			e_{xy}	h_{xz}					
14			e_{yx}	e_{yz}				e_{yz}			e_{yx}			h_{yz}				
15					e_{zy}	e_{zx}	e_{zy}			e_{zx}					h_{zx}			
16				f_{zx}	$-f_{yx}$		f_{yx}	$-f_{zx}$								j_{zx}		
17		$-f_{zy}$				f_{xy}			f_{zy}	$-f_{xy}$							j_{zy}	
18	f_{yz}		$-f_{xz}$								f_{xz}	$-f_{yz}$						j_{xz}
19	k_{xy}	k_{xz}							k_{xz}			k_{xy}	l_{xz}					
20			k_{yx}	k_{yz}				k_{yz}			k_{yx}			l_{yz}				
21					k_{zy}	k_{zx}	k_{zy}			k_{zx}					l_{zx}			
22				$-m_{zx}$	m_{yx}		$-m_{yx}$	m_{zx}								n_{zx}		
23		m_{zy}				$-m_{xy}$			$-m_{zy}$	m_{xy}							n_{zy}	
24	$-m_{yz}$		m_{xz}								$-m_{xz}$	m_{yz}						n_{xz}

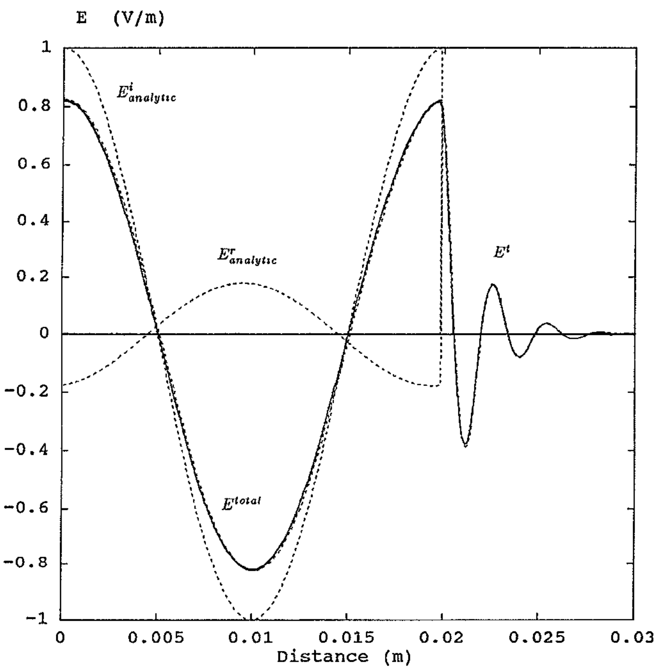

Fig. 1. Transverse electromagnetic wave normally incident on a lossy half space; $f = 15GHz$, $\epsilon_r = 10 - j3$, and $\mu_r = 5 - j1$ for $x \geq 19.875mm$.

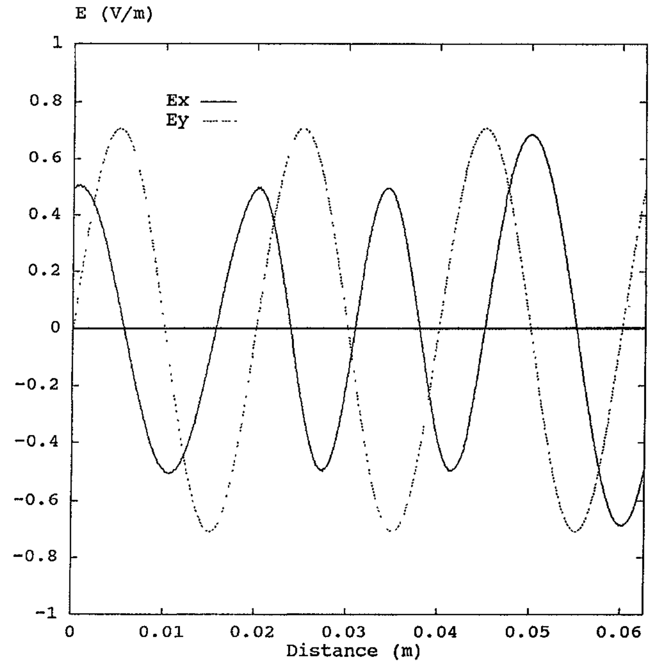

Fig. 2. Counterclockwise, circularly polarized wave normally incident on a birefringent lens; $f = 15GHz$, $\epsilon_{xx,r} = 2$, and $\epsilon_{yy,r} = 1$ for $19.875mm \leq x \leq 44mm$.

along with the various nodes (HSCN I, HSCN II, and Johns's SCN), given as the solid lines, and the analytic solution, given as the dashed lines.

B. Birefringent Lens

A birefringent lens is an anisotropic device used to change the polarization of light [10]. Fig. 2 shows the passage of a circularly polarised wave through a birefringent half-wave plate, calculated using the TLM method and the three nodes. The incident counterclockwise, (CCW) circularly polarized wave is composed of E_x and E_y components having equal amplitudes $E_{x,max} = E_{y,max} = 1/\sqrt{2}$ but differing phase shifts such that $\phi_x - \phi_y = -\pi/2$. We note that the E_y component of the wave passes through the lens without distortion; this is expected since $\epsilon_{yy,r} = 1$. The E_x component, however, is transmitted through the lens with a phase shift. Upon emergence from the lens at $x = 44mm$, we note that $\phi_x - \phi_y = \pi/2$, thus producing a clockwise (CW)-polarized wave. The E_x component of the wave suffers multiple reflections at the interfaces with the lens. These multiple reflections reduce the amplitude of the emerging component producing a slightly elliptical CW polarization at the output of the lens. Usually, a thicker birefringent plate is constructed from a material having $\epsilon_{xx,r}$ closer to air.

IV. Conclusion

A new hybrid symmetrical condensed TLM node has been presented along with a reformulation of the existing hybrid node to include anisotropic media. Results computed using the TLM method along with the two hybrid nodes and Johns's node have been obtained. It has been found that all three nodes provide similar results and that they agree well with analytic solutions.

References

[1] P. B. Johns, "A Symmetrical Condensed Node for the TLM Method," *IEEE Trans. Microwave Theory Tech.*, vol. MTT-35, pp. 370–377, Apr. 1987.
[2] D. A. Al-Mukhtar and J. E. Sitch, "Transmission-Line Method With Irregularly Graded Space," *IEE Proc., part H*, vol. 128, pp. 299–305, Dec. 1981.
[3] R. Scaramuzza and A. J. Lowery, "Hybrid Symmetrical Condensed Node for the TLM Method," *Electron. Lett.*, vol. 28, pp. 1947–1949, Nov. 1990.
[4] P. Naylor and R. A. Desai, "New Three Dimensional Symmetrical Condensed Node For Solution of Electromagnetic Wave Problems by TLM," *Electron. Lett.*, vol. 26, pp. 492–494, Mar. 1990.
[5] F. J. German, G. K. Gothard, and L. S. Riggs, "Modelling of Materals With Electric and Magnetic Losses With the Symmetrical Condensed TLM Method," *Electron. Lett.*, vol. 26, pp. 1307–1308, Aug. 1990.
[6] P. Naylor and R. Ait-Sadi, "Simple Method for Determining 3-D TLM Nodal Scattering in Nonscalar Problems," *Electron. Lett.*, vol. 28, pp. 2353–2354, Dec. 1992.
[7] P. Naylor and R. Ait-Sadi, "Reply to Comments on Simple Method for Determining 3-D TLM Nodal Scattering in Nonscalar Problems," *Electron. Lett.*, vol. 29, pp. 1056–1057, June 1993.
[8] V. Trenkic, C. Christopoulos, and T. M. Benson, "Simple and Elegant Formulation of Scattering in TLM Nodes," *Electron. Lett.*, vol. 29, pp. 1651–1652, Sept. 1993.
[9] R. Scaramuzza, P. Naylor, and C. Christopoulos, "Numerical Simulation of Field-to-Wire Coupling Using Transmission Line Modelling," in *Proc. Int. Conf. Computations in Electromagnetics*, IEE Conf. Pub. no. 350, pp. 63–66, 1991.
[10] A. Yariv and Y. Pochi, *Optical Waves in Crystal, Propagation and Control of Laser Radiation.* Wiley Interscience, 1984.